From motivation to action: action cost better predicts changes in pre-movement beta-band activity than speed

Emeline Pierrieau, Bastien Berret, Jean-François Lepage, Pierre-Michel Bernier

Title: From motivation to action: action cost better predicts changes in pre-movement beta-band activity than speed

Abbreviated title: Beta activity is better explained by action cost than speed

Authors: Emeline Pierrieau [*1], Bastien Berret [2], Jean-François Lepage [1,3], Pierre-Michel Bernier [4].

Affiliations: [1] Programme de Physiologie, Faculté de Médecine et des Sciences de la Santé, Université de Sherbrooke, Sherbrooke, Québec J1H 5N4, Canada. [2] Université Paris-Saclay, CIAMS, 91405 Orsay, France; CIAMS, Université d'Orléans, 45067 Orléans, France; Institut Universitaire de France, Paris, France. [3] Département de Pédiatrie, Faculté de Médecine et des Sciences de la Santé, Université de Sherbrooke, Sherbrooke, Québec J1H 5N4, Canada. [4] Département de Kinanthropologie, Faculté des Sciences de l'Activité Physique, Université de Sherbrooke, Sherbrooke, Québec J1K 2R1, Canada.

Corresponding author email: emeline.pierrieau@u-bordeaux.fr

Number of pages: 43

Number of figures: 5 *Number of tables:* 1

Number of words:

- *Abstract: 249*
- *Introduction: 648*
- *Discussion: 1499*

Conflict of interest statement: The authors declare no competing financial interests.

Acknowledgments: We thank François Thénault for his help in developing the scripts used for the experiment and Dominique Delisle-Godin for her help in collecting data. This work was supported by the Natural Sciences and Engineering Research Council of Canada Grant 418589.

Abstract

Although pre-movement beta-band event-related desynchronization (13-30 Hz; β-ERD) from sensorimotor regions is modulated by movement speed, current evidence does not support a strict monotonic association between the two. Given that β-ERD is thought to increase information encoding capacity, we tested the hypothesis that it might be related to the expected neurocomputational cost of movement, here referred to as action cost. Critically, action cost is greater both for slow and fast movements as compared to a medium or "preferred" speed. Thirty-one right-handed participants performed a speed-controlled reaching task while recording their EEG. Results revealed potent modulations of β power as a function of speed, with β-ERD being significantly greater both for movements performed at high and low speeds as compared to medium speed. Interestingly, medium-speed movements were more often chosen by participants than low- and high-speed movements, suggesting that they were evaluated as less costly. In line with this, modeling of action cost revealed a pattern of modulation across speed conditions that strikingly resembled the one found for β-ERD. Indeed, linear mixed models showed that estimated action cost predicted variations of β-ERD significantly better than speed. This relationship with action cost was specific to β power, as it was not found when averaging activity in the mu (μ; 8-12 Hz) and gamma (γ; 31-49 Hz) bands. These results demonstrate that increasing β-ERD may not merely speed up movements, but instead facilitate the preparation of high- and low-speed movements through the allocation of additional neural resources, thereby enabling flexible motor control.

Significance statement

Heightened β activity has been associated with movement slowing in Parkinson's disease and modulations of β activity are commonly used to decode movement parameters in brain-computer interfaces. Here we show that pre-movement β activity is better explained by the neurocomputational cost of the action rather than its speed. Instead of being interpreted as a mere reflection of changes in movement speed, pre-movement changes in β activity might therefore be used to infer the amount of neural resources that are allocated for motor planning.

Introduction

Unveiling the neurophysiological basis and functional role of brain activity in the beta-band (β; 13-30 Hz) is of particular interest to basic motor control scientists as well as clinicians because of its characteristic pattern of modulation with movement, described as event-related desynchronization (ERD; Pfurtscheller and Lopes da Silva, 1999), and its specific alteration in neurological disorders such as Parkinson's disease (PD; Jenkinson and Brown, 2011). Although numerous studies have attempted to link these movement-related changes in β power to behavior, the evidence so far has been inconsistent, making its functional interpretation still an area of active debate (Engel and Fries, 2010; Brittain and Brown, 2014; Spitzer and Haegens, 2017).

β power has often been related to motor activity: the amplitude of β-ERD has been positively correlated with corticospinal excitability (Takemi et al, 2013) and with the activation level of the sensorimotor cortex (Yuan et al, 2010), and β power from local field potentials of the subthalamic nucleus has been related to the encoding of motor effort (Tan et al, 2015). Furthermore, non-invasive neurostimulation studies have shown that specifically increasing β-band activity tends to decrease movement speed (Pogosyan et al., 2009; Wach et al, 2013). The most striking evidence of a significant association between β power and movement speed comes from patients suffering from PD. PD is notably characterized by motor symptoms such as bradykinesia (i.e., movement slowing; Bloem et al., 2021). β power is increased in PD, and can be attenuated with treatments (Kühn et al., 2006; Ray et al., 2008). The greater the decrease in β power, the greater the improvement in bradykinesia (Jenkinson and Brown, 2011), making β power a promising therapeutic target. Although PD treatment most often targets β power at the subcortical level, there is evidence of abnormalities in cortical β power as well, such as an attenuation of pre-movement β-ERD (Heinrichs-Graham et al., 2014). Still, the relationship

between β power and movement speed does not appear monotonic, as several studies have reported no significant difference in β-ERD between slow and fast movements (Stancák and Pfurtscheller, 1995; Zhang et al., 2020; see Kilavik et al., 2013 for a review).

From a functional perspective, several studies have provided evidence in favor of a specific role of β activity in regulating computational power through (de)synchronization of neuronal populations within sensorimotor regions (Brittain et al, 2014), being proposed to be related to top-down interactions (Fries, 2015) and expressing the influence of priors on newly formed neuronal assemblies (Betti et al, 2021). Put another way, β power would decrease in order to augment neurocomputational power required for information processing (Brittain and Brown, 2014), as exemplified by greater β-ERD when increasing cognitive demand during motor planning (Grent-'t-Jong et al., 2013; Wiesman et al., 2020). One intriguing conjecture is that β-ERD amplitude may increase as a function of the neurocomputational cost of the movement being prepared, referred to herein as action cost. Action cost can be represented as the sum of a biomechanical cost, which increases with movement speed, and a temporal cost, which decreases with movement speed (Berret and Jean, 2016; Shadmehr et al., 2016). This leads to a u-shaped action cost function, the minimal value of which has been shown to predict the preferred speed of participants in various motor contexts (Berret and Jean, 2016). According to this hypothesis, β-ERD amplitude would thus vary non-monotonically with movement speed, being greater both for slow and fast movements in comparison to movements performed at medium (i.e., near-preferred) speed.

We tested this hypothesis by using a speed-controlled reaching paradigm while applying computational modeling to estimate the associated action cost. Results revealed that β-ERD amplitude varied non-monotonically with movement speed, in a manner that was strikingly well predicted by estimated action cost. These results invite to rethink the interpretation of β power

as a marker of cortical resources allocated for movement instead of a mere correlate of movement kinematics such as speed.

Materials and methods

1. Participants

Thirty-one participants (15 females, 23 ± 3 (mean ± SD) years old) were recruited for this study. All of them were right-handed based on self-report. They had normal or corrected-to-normal vision and were free of any known neurological or psychiatric condition. All participants gave their informed written consent and received a 30$ CAD compensation. All procedures were approved by the local ethics committee. The experiment conformed to the standards set by the 1964 Declaration of Helsinki.

2. Experimental task

2.1. Setup

The experimental setup consisted of a table supporting a 20-inch computer monitor that projected visual stimuli onto a mirror positioned horizontally in front of the participants. The monitor (Dell P1130 20-inch monitor; resolution: 1024 × 768; refresh rate: 150 Hz) was mounted face down 29 cm above the mirror with the latter positioned 29 cm above the table surface. Participants' movements were recorded with an acquisition frequency of 100 Hz, using a two-joint manipulandum composed of two lightweight metal rods with a potentiometer at the hinges of the manipulandum. Participants performed their movements by grasping a handle located at the mobile end of the manipulandum with their right hand and sliding it over the table. The position of the handle (and thus participants' hand) was shown to participants using a cursor on the monitor. This provided constant visual feedback of participants' hand position, similar to a computer mouse. A 64-electrode actiCAP (extended 10/20 system, Brain Products) was positioned on participants' head to record scalp electroencephalography (EEG). This was done by measuring the head dimensions in the sagittal and frontal planes to localize the vertex

and positioning the reference electrode (FCz) over it. The EEG data were acquired using the BrainVision Recorder software 2.0 (Brain Products) with a sampling rate of 500 Hz.

2.2. Overview

Participants were seated in front of the table and asked to reach a visual target (cyan-filled circle, diameter = 3 cm) with their right hand. Visual stimuli were presented using Psychtoolbox on MATLAB (MathWorks). Trials were initiated by placing the cursor (white filled circle, diameter = 0.6 cm) on a starting point (light gray filled circle, diameter = 0.6 cm) located at the center of the screen. Participants were told to place their chin on a small support, to keep their right arm in contact with the surface of the table, and to minimize postural changes during the experiment. The target was presented either on the right side of the screen (60°, Rt) at a distance of 10 cm from the starting point, or on the left side of the screen (150°, Lt) 6 cm away from the starting point. These positions were chosen to ensure that the maximal peak velocity participants could reach was significantly different for each target. Indeed, maximal peak velocity increases with distance (Gottlieb et al., 1989) as well as with the biomechanical constraints of the movement (Gordon et al., 1994). The biomechanical constraints of a reaching movement depend upon movement direction and can be represented as an ellipse of mobility of the arm, due to changes in its effective mass because of its inertial properties (Shadmehr et al., 2016). The major axis of the ellipse of mobility corresponds to the directions associated with the lowest effective mass of the arm, and thus the easiest and fastest to reach. Conversely, the minor axis of the ellipse corresponds to the directions in which the effective mass of the arm is the highest, resulting in more difficult and slower movements. In the present task, Rt was located on the major axis and Lt on the minor axis. Hence, maximal velocity was expected to be significantly higher for movements oriented toward Rt than Lt.

2.3. Trial timeline

Trial timeline is illustrated on Figure 1A. Trials started with the display of a white fixation cross (1.1 x 1.1 cm) 4 cm above the starting point on the screen. Once the cursor was placed on the starting point, participants were required to keep their gaze on the fixation cross for the entire trial duration. They were also asked to minimize eye blinks until they reached the target to avoid artifacts in the EEG signal during the period of interest. After a 2 s delay, the target appeared on the screen. A gauge (6.6 x 1.3 cm) centered on the fixation cross appeared simultaneously to the target. The filling level of the gauge was informative of the speed at which participants would have to perform their movement toward the target: one-quarter filling indicated a slow speed (Low), half filling a medium speed (Med), and three-quarter filling a fast speed (High) (see Figure 1B and next section for details about speed requirements). An auditory go cue occurred 2 s after target and gauge appearance, signaling that the movement could be initiated. Participants were asked to start their movement quickly after they heard the go cue. If participants initiated their movement before the go cue, an error message was displayed for 1 s ("false start") and the trial was automatically re-run. Once the movement ended, all stimuli disappeared and were replaced by visual feedback of whether the speed criterion was reached or not in the form of a message ("well done!" if the speed criterion was attained, or the difference in cm/s between the peak velocity reached during the trial and the speed criterion if it was not attained). Movements were required to end inside the chosen target to ensure accuracy and thus comparability of trials across conditions. In case the target was missed, an error message was displayed for 1 s ("target missed") and the trial was re-run. Whatever the visual feedback, it was replaced after 1 s by the appearance of the white fixation cross with the starting point and the cursor. The next trial started when the cursor was placed inside of the starting point. Participants were encouraged to take a break between trials by not immediately replacing the cursor inside of the starting point if they felt the need to move their eyes, head or body, or if they wanted to rest for a few seconds. The experiment was organized

in 4 blocks of 60 trials, which comprised 2 blocks of trials requiring movements toward Rt, and 2 blocks of movements directed to Lt. The speed conditions varied pseudo-randomly throughout trials in one block so that a same speed condition was not presented twice in a row and each block comprised 20 trials of each speed condition.

Participants familiarized with the experimental task and their maximal speeds were estimated before doing the trials described above. Participants first performed 10 movements toward each target at a comfortable pace, organized in blocks of 5 trials presented in an alternating order (5 Rt trials, 5 Lt trials, 5 Rt trials and 5 Lt trials), to familiarize with the setup. Then, they performed 60 trials in which they were asked to reach the presented target as fast as possible (30 Rt trials followed by 30 Lt trials) to estimate their maximal speeds. Rt and Lt trials were separated by a short break that ended when participants felt rested, to avoid an effect of physical fatigue on motor performance (even though fatigue was also minimized on a single-trial basis by allowing participants to delay the start of the next trial by not immediately placing their cursor inside of the starting point as previously explained). Finally, participants familiarized with the different speed criteria by performing trials in each speed condition. More precisely, trials from a given speed condition were repeated until achieving the correct speed five times (not necessarily back-to-back). All of these familiarization and "maximal speed" trials were organized the same way as those in the main experiment, except that no gauge was displayed in the first familiarization and maximal speed trials.

2.4. Experimental conditions and their related hypotheses

Speed criteria were defined in order to create conditions requiring different peak velocities but similar relative effort (i.e., difference from maximal peak velocity). 6 velocity criteria (2 Targets x 3 Gauges) were used in total: for movements toward Rt 120 cm/s when the gauge had a three-quarter filling (HighRt), 95 cm/s when the gauge was half-filled (MedRt), and 70 cm/s

when the gauge had a one-quarter filling (LowRt); for movements toward Lt 60 cm/s when the gauge had a three-quarter filling (HighLt), 40 cm/s when the gauge as half-filled (MedLt) and 20 cm/s when the gauge had a one-quarter filling (LowLt) (Figure 1B). During trials, these speed criteria were considered as attained if the peak velocity of the movement was comprised in an interval of ± 5 cm/s centered on the speed criterion of the corresponding condition. In addition, to ensure significant differences in movement speed across conditions, these criteria were set so that the High speed criteria was to be close to the maximal speed participants could reach for each target considering differences in amplitude and inertial anisotropy (Gordon et al., 1994; Shadmehr et al., 2016). To verify this assumption, participants were first asked to perform 30 reaching movements toward each target as fast as possible ("maximal speed" trials defined before) and the average maximal peak velocity was then compared to the average peak velocity in High trials a posteriori (see Results section). Therefore, the present design allowed to test the respective influences of speed and effort on β power. Indeed, if β power is influenced by absolute movement speed, then both an effect of Gauge and Target should be expected considering that the two factors significantly influence peak velocities (Figure 1C, left panel), whereas if β power is influenced by the movement speed relative to its maximal value as a measure of expected effort (Tan et al., 2015), then only a significant effect of Gauge should be found in spite of the significantly different speed ranges reached for each target (Figure 1C, middle panel). Finally, modeling work has demonstrated that optimal/preferred movement speed could be selected based on the joint minimization of a trajectory or metabolic cost that increases as movement speed increases, and of a cost of time that increases as movement speed decreases (Berret and Jean, 2016). Based on this model, the relationship between movement speed and action cost is not linear but instead follows a u-shaped curve. As a consequence, β power may vary non-linearly with speed, and therefore decrease in High and Low conditions as compared to Med (Figure 1C, right panel).

[Insert Figure 1]

3. Data analysis

3.1. Behavior

Hand position was estimated in real-time with the coordinates of the cursor recorded with the two potentiometers located on the manipulandum. Recorded signals were sampled at 100 Hz and were low-pass filtered at 10 Hz using a second-order Butterworth filter. Real-time velocities were determined for each trial using numerical differentiation. The maximal value of these real-time velocities was considered as the peak velocity. Movement onset was defined as the first time point at which velocity exceeded 5% of the peak velocity and movement end as the first time point at which velocity fell below 5% of this same peak velocity (Berret and Jean, 2016). RTs were calculated as the latency separating the auditory go cue and movement onset, and MTs as the latency separating movement onset and movement end. Trials in which the cursor was located outside of the presented target at the time of movement end were considered as missed-target trials and were not included in the analysis (representing 2.35% trials). In the same vein, trials in which participants initiated their movement before the go cue occurred were removed from the analysis (representing 1.06% trials). Note that removing those trials did not affect the number of trials per condition included in the analysis because, as previously mentioned, any missed target or false start was automatically re-run during the experiment.

3.2. EEG

All EEG data were processed offline using custom MATLAB codes and functions from EEGLAB (Delorme and Makeig, 2004) and Fieldtrip (Oostenveld et al., 2011). First, a bandpass filter between 1 and 80 Hz was applied on raw EEG data, with a 59–61 Hz notch filter to attenuate electrical noise. The signal was re-referenced to the average scalp potential. The

data were then segmented into epochs of 4.5 s duration locked around the occurrence of the auditory go cue (3 s before to 1.5 s after go cue). The period of interest corresponded to the 2 s delay separating stimuli onset (i.e., target and gauge appearance) and the go cue. Independent component analysis (ICA) was applied to EEG data using the runica algorithm from the EEGLAB toolbox, in order to remove artifactual EEG activity associated with eye and head movements and other sources of noise (Jung et al., 2000). A surface Laplacian transform was applied on the EEG data with artifactual components removed, using the erplab plugin from EEGLAB. The EEG signal was then downsampled to 125 Hz to reduce computation time for time–frequency decomposition. The latter was performed afterward, using Morlet wavelets (4–45 Hz with 1 Hz steps). The wavelet cycles were increased at each frequency in 0.1 steps (starting from 3 to 10.6 cycles) to ensure a balance between sufficient temporal resolution at lower frequencies and frequency resolution at higher frequencies. Finally, the data were normalized for each condition by measuring the absolute change from the average power during the 500 ms preceding the delay period (0.5 to 1 s of the total epoch). The amplitude of β-ERD was quantified as the absolute value of average β power recorded during the delay period separating the stimulus onset and the auditory go cue.

3.3. Action cost modeling

Action costs were computed from the sum of estimated trajectory cost and cost of time following the method of Berret and Jean (2016). In short, the trajectory cost was based on the distance to the target, the joint torque and the hand jerk. It thus reflects accuracy, smoothness, and effort aspects of the reaching movement, and depends on task parameters (e.g., angle and amplitude of the presented target, anthropometry, starting position of the arm). In contrast, the cost of time rests on the quantification of the affine relationship between movement amplitude and duration that is characteristic of self-paced reaching movements and hence can be inferred

from experimental data (see Methods section of Berret and Jean, 2016 for details). Therefore, the model enables the computation of action cost as a function of movement duration. The "optimal" MT (i.e., the one associated with the lowest action cost) is supposed to predict the average MT in a context where participants perform self-paced movements, corresponding to their "preferred" MT. Here, because there was no self-paced reaching condition, the slope of this relationship was retrieved from the data of Young et al. (2009), who used a similar reaching task with high temporal constraints. The intercept was adjusted to predict the average MT found in Med, separately for movements directed to Rt and Lt. In other words, the cost of time was set based on a movement duration-amplitude relationship that predicted MTs corresponding to the ones found in Med at the amplitude used in the present experimental task. Average MTs in Med were selected because analysis of participants' speed distributions in the task showed that average speeds that were the most often chosen (thereby the closest estimates of "preferred" speeds) were not significantly different from average speeds in Med, both for movements directed to Rt and Lt (see Results). Peak velocities associated with MTs toward each target were computed from the predicted optimal velocity profiles, which were bell-shaped similarly to minimum jerk profiles (Flash and Hogan, 1985; Shadmehr et al., 2016). Action costs were therefore estimated both as a function of MTs and their associated peak velocities, and then normalized between 0 and 1 across velocity ranges centered on the minimal value of the cost functions (i.e., estimated preferred/optimal peak velocity), separately for movements directed to Lt and Rt. These velocity ranges were set to include all measured peak velocity values toward each target.

3.4. Experimental design and statistical analyses

An intra-participant design was used, so that all the factors included in the statistical analyses were within-participant. 2 x 3 repeated-measures ANOVAs were performed using

Target (Rt, Lt) and Gauge (Low, Med, High) as factors on peak velocities, RTs, MTs, absolute error (i.e., average distance between movement endpoint and target center), standard deviation of the absolute error, probability of reaching the speed criterion, as well as β, μ and γ power and estimated action costs. Additional analyses with ANOVAs including Target, Gauge and Block (1 and 2) as factors were conducted to assess whether the main results remained throughout blocks of trials. Action costs were estimated based on average peak velocities across participants and conditions (Gauge), separately for the two target positions (Target) that were used because a distinct model was fitted to each of them (see previous section), considering that maximal and preferred speeds differed across targets (see Results section). T-tests were used for post-hoc analysis, with a Bonferroni correction applied to p-values for multiple comparisons. Effect sizes are reported as partial eta squared (η^2p) for ANOVAs and Cohen's d (d) for t-tests. Cluster-based permutation tests were performed to identify electrodes associated with significant modulations of β, μ and γ power across experimental conditions using functions from Fieldtrip (Oostenveld et al., 2011). Monte Carlo permutations (n = 1000) were used to determine p-values for each cluster. A cluster-level correction was set to control for multiple comparisons, using the sum of t-values. A cluster was defined as at least two neighboring electrodes (located less than 4 cm from each other) showing statistically significant t-values. General linear mixed models (GLMMs) were used to evaluate which of peak velocity or estimated action cost best explained the variance in β power. Probability density functions of distributions of peak velocities were estimated using kernel distributions (*ksdensity()* command in Matlab), separately for each target and participant. Kernel distributions are non-parametric representations of probability density distributions, and are thus suited to estimate probability density distributions from multimodal distributions such as the ones that were expected from the experimental manipulation of peak velocities in the present task. Average estimated

preferred peak velocities were computed as the mean of the peak velocities corresponding to the maximal probability density functions across participants, separately for each target.

All statistical tests were computed using Jamovi v. 1.2.27 (the jamovi project, 2019, computer software, retrieved from https://www.jamovi.org), a software that implements R statistical language (R Core Team, 2018, R: a language and environment for statistical computing, computer software, retrieved from https://www.cran.r-project.org/).

Results

Briefly, the experimental task consisted of presenting a target along with a gauge, indicating where to reach and at which speed. The visual stimuli appearance was followed by a delay period before the occurrence of an auditory go cue (Figure 1A). Two different target positions (Target: Rt, Lt) and three different filling levels of the gauge (Gauge: Low, Med, High) were used across trials. Critically, each filling level of the gauge was associated with a different speed criterion based on peak velocity values. These speed criteria were set so that the speed required for the highest filling of the gauge (High) was close to the maximal speed participants could reach for movements directed to each target separately (see Figure 1B for a summary of the experimental conditions and their associated speed criterion and Methods section for details). This experimental design allowed to test three main hypotheses about the association between β-ERD and speed: if β-ERD is modulated as a function of absolute speed, then main effects of both Target and Gauge should be expected considering the distinct speeds reached across conditions (Figure 1C, left panel). Alternatively, if β-ERD is modulated as a function of speed relative to its maximum, only a main effect of Gauge should be observed (Figure 1C, middle panel). Finally, if β-ERD is modulated by action cost instead of speed, only a main effect of Gauge should be expected and β-ERD should be increased in both Low and High as compared to Med given that increasing and decreasing speed represents an additional cost (Figure 1C, right panel, see Methods for details).

1. Movement speed

The first part of the analysis consisted in verifying that movement speed was effectively modulated in the present task. Peak velocities were indeed strongly influenced both by Target ($F(1,30) = 2264$, $p < 10^{-10}$, $\eta^2p = 0.99$) and Gauge ($F(2,60) = 843$, $p < 10^{-10}$, $\eta^2p = 0.97$) with a significant interaction between the two ($F(2,60) = 140$, $p < 10^{-10}$, $\eta^2p = 0.82$). Post-hoc analysis

showed that peak velocities were significantly increased when comparing MedRt to LowRt ($t(30) = 25.7$, $p < 10^{-10}$, $d = 4.62$) and HighRt to MedRt ($t(30) = 18.0$, $p < 10^{-10}$, $d = 3.23$), as well as when comparing MedLt to LowLt ($t(30) = 27.0$, $p < 10^{-10}$, $d = 4.85$) and HighLt to MedLt ($t(30) = 17.8$, $p < 10^{-10}$, $d = 3.20$). The effect of Target on peak velocities was also strong, with significant increases found when comparing LowRt to LowLt ($t(30) = 34.6$, $p < 10^{-10}$, $d = 6.22$), MedRt to MedLt ($t(30) = 39.1$, $p < 10^{-10}$, $d = 7.02$) and HighRt to HighLt ($t(30) = 51.2$, $p < 10^{-10}$, $d = 9.20$). The average peak velocities were as follows: 71.0 ± 8.0 cm/s for LowRt, 97.0 ± 8.1 cm/s for MedRt, 124.4 ± 9.4 cm/s for HighRt, 24.0 ± 8.0 cm/s for LowLt, 42.4 ± 6.3 cm/s for MedLt and 58.4 ± 6.2 cm/s for HighLt (Figures 2A and 2B).

Separating data across blocks (2 levels: Block 1 and Block 2) does not significantly change this result. Indeed, this additional analysis showed significant effects of Target ($F(1,30) = 2264.4$, $p < 10^{-15}$, $eta^2p = 0.99$) and Gauge ($F(1,30) = 842.9$, $p < 10^{-15}$, $eta^2p = 0.97$) but not of Block ($F(1,30) = 0.0$, $p = 0.862$, $eta^2p = 0.00$). Significant interactions were found between Target and Gauge ($F(2,60) = 139.9$, $p < 10^{-15}$, $eta^2p = 0.82$) as well as Gauge and Block ($F(2,60) = 7.5$, $p = 0.001$, $eta^2p = 0.20$), but no interaction was found between Target and Block ($F(1,30) = 0.2$, $p = 0.662$, $eta^2p = 0.01$), nor Target, Gauge and Block ($F(2,60) = 2.4$, $p = 0.100$, $eta^2p = 0.07$). Post-hoc analysis of the interaction between Gauge and Block revealed that peak velocity was slightly increased in High in Block 2 as compared to Block 1 ($t(30) = 3.2$, $p = 0.010$, $d = 0.57$) by 1.89 ± 1.21 cm/s (mean ± 95% CI). No significant difference in peak velocity between Block 1 and Block 2 was found in Med ($t(30) = 0.7$, $p = 1.00$, $d = 0.12$) nor in Low ($t(30) = 2.2$, $p = 0.117$, $d = 0.39$). Although participants appear to have increased their speed in High in Block 2 as compared to Block 1, this effect appeared relatively modest considering the speed difference induced (less than 2 cm/s) in comparison to the speed difference between conditions (around 10 times greater; mean difference of 22.2 cm/s between Low and Med and 21.7 cm/s between Med and High).

The probability of performing the movement within the speed criteria was strongly impacted by Target ($F(1,30) = 68.9$, $p = 10^{-9}$, $eta^2p = 0.70$) and to a lesser extent by Gauge ($F(2,60) = 4.9$, $p = 0.011$, $eta^2p = 0.14$) and there was no significant interaction between the two ($F(2,60) = 2.6$, $p = 0.085$, $eta^2p = 0.08$). Post-hoc analysis revealed that the probability of reaching the speed criterion was higher for movements directed to Lt than Rt ($t(30) = 8.3$, $p = 10^{-9}$, $d = 1.49$) and for movements performed in High than Low, though with a lower effect size ($t(30) = 2.7$, $p = 0.030$, $d = 0.49$). No significant difference in the probability of achieving the speed criteria was found between Low and Med ($t(30) = 1.6$, $p = 0.369$, $d = 0.29$), or between Med and High ($t(30) = 1.8$, $p = 0.240$, $d = 0.33$).

Participants were first asked to perform their movements at maximal speed to ensure that their average maximal speeds for movements directed to each target were close to the speed criteria used in High conditions (see Methods for details). The analysis of these trials confirmed that maximal peak velocities were significantly greater for movements directed to Rt in comparison to movements directed to Lt ($t(30) = 23.5$, $p < 10^{-10}$, $d = 4.23$). The average maximal peak velocity found for movements directed to Lt was not significantly different from the average peak velocity in HighLt ($t(30) = 0.2$, $p = 1.0$, $d = 0.04$, mean difference = 0.2 cm/s, $BF_{10} = 0.20 \pm 0.03$, moderate evidence for H0). However, the average maximal peak velocity found for movements toward Rt were slightly but significantly lower than the average velocity in HighRt ($t(30) = -3.0$, $p = 0.010$; $d = -0.54$; mean difference = -8.8 cm/s, $BF_{10} = 7.80 \pm 1.42e\text{-}6$, moderate evidence for H1). This suggests that the velocity criteria used in HighRt and HighLt were close to the maximal speed participants could reach for movements directed toward those targets but might have been more challenging for HighRt because its velocity criterion slightly exceeded the maximal speed expressed by participants.

As could be expected from these results, overall response time was significantly impacted by manipulations of peak velocities. Indeed, a significant influence of Target was found on MTs ($F(1,30) = 123.8$, $p < 10^{-10}$, $\eta^2p = 0.80$) as well as a significant influence of Gauge ($F(2,60) = 164.2$, $p < 10^{-10}$, $\eta^2p = 0.85$) and an interaction between the two ($F(2,60) = 64.3$, $p < 10^{-10}$, $\eta^2p = 0.68$). Post-hoc analysis showed similar results as for peak velocities with increased MTs in LowRt as compared to MedRt ($t(30) = 16.9$, $p < 10^{-10}$, $d = 3.03$) and in MedRt as compared to HighRt ($t(30) = 12.0$, $p < 10^{-10}$, $d = 2.16$), as well as in LowLt as compared to MedLt ($t(30) = 10.1$, $p = 10^{-10}$, $d = 1.81$) and in MedLt as compared to HighLt ($t(30) = 13.5$, $p < 10^{-10}$, $d = 2.43$). MTs were also significantly increased in LowLt as compared to LowRt ($t(30) = 9.4$, $p < 10^{-9}$, $d = 1.69$), in MedLt as compared to MedRt ($t(30) = 13.1$, $p < 10^{-10}$, $d = 2.35$) and in HighLt as compared to HighRt ($t(30) = 11.6$, $p < 10^{-10}$, $d = 2.08$; Figure 2C).

In contrast, RTs were not significantly impacted by Target ($F(1,30) = 0.1$, $p = 0.794$, $\eta^2p = 0.00$) but by Gauge ($F(2,60) = 17.0$, $p = 10^{-6}$, $\eta^2p = 0.36$) with a significant interaction between the two ($F(2,60) = 6.4$, $p = 0.003$, $\eta^2p = 0.18$). Post-hoc analysis showed that RTs were significantly increased in Low as compared to High ($t(30) = 4.4$, $p = 10^{-4}$, $d = 0.79$) and Med ($t(30) = 3.1$, $p = 0.014$, $d = 0.55$), and in Med as compared to High ($t(30) = 5.9$, $p = 10^{-5}$, $d = 1.06$). The interaction effect comes from the fact that the difference in RTs between movements directed to Rt and Lt tended to change with the filling of the gauge but remained non significantly different across Gauge levels (LowRt vs LowLt: $t(30) = -1.8$, $p = 0.258$, $d = -0.32$; MedRt vs MedLt: $t(30) = 1.2$, $p = 0.771$, $d = 0.21$; HighRt vs HighLt: $t(30) = 0.3$, $p = 1.0$, $d = 0.05$; Figure 2D).

Finally, the absolute error (i.e., average distance between movement endpoint and target center) was significantly higher for movements directed to Rt as compared to movements directed to Lt (main effect: $F(1,30) = 33.4$, $p = 10^{-6}$, $eta^2p = 0.53$; post-hoc: $t(30) = 5.8$, $p = 10^{-}$

^{6}, d = 1.04) and was increased in High in comparison to both Med and Low (main effect: F(2,60) = 25.4, p = 10^{-8}, eta²p = 0.46; post-hoc: High vs Low: t(30) = 5.7, p = 10^{-5}, d = 1.03; High vs Med: t(30) = 6.0, p = 10^{-5}, d = 1.07; Med vs Low: t(30) = 1.7, p = 0.318, d = 0.30) without significant interaction between Target and Gauge (F(2,60) = 1.5, p = 0.225, eta²p = 0.05). The standard deviation of the absolute error showed similar trends by monotonically increasing with speed (Target/main effect: F(1,30) = 40.9, p = 10^{-7}, eta²p = 0.58; Target/post-hoc: Rt vs Lt: t(30) = 6.4, p = 10^{-7}, d = 1.15; Gauge/main effect: F(2,60) = 28.9, p = 10^{-9}, eta²p = 0.49; Gauge/post-hoc: High vs Low: t(30) = 8.2, p = 10^{-8}, d = 1.47; High vs Med: t(30) = 3.4, p = 0.006, d = 0.61; Med vs Low: t(30) = 4.1, p = 0.001, d = 0.73; Target*Gauge: F(2,60) = 0.2, p = 0.853, eta²p = 0.01). Critically, these differences in movement accuracy had little impact on task performance as the diameter of the target was set relatively large (3 cm) so that participants failed to end their movements inside of the target in only 2.35 % of trials, which were removed from the analysis and re-run (see Methods for details).

[Insert Figure 2]

2. β power

Cluster-based permutation tests comparing the fastest (HighRt) to the slowest (LowLt) conditions revealed a significant negative cluster (t_{sum} = -4478.5, p = 0.001) 1.4 s to 0 s before the go cue. As can be seen in Figure 3A, the cluster appeared over the left fronto-central scalp sites, centered around electrodes C3, C1, FC3 and FC1. Given that motor β-ERD is commonly quantified around these electrodes (e.g., Fischer et al., 2018; Haddix et al., 2021; Chen and Kwak, 2022), as they overlay (pre)motor regions (Scrivener et al., 2021), β-ERD was computed as the mean signal from those four electrodes. The visual depiction of the time course of β

power indeed showed distinct modulations across conditions during the delay period preceding the go cue (Figure 3B). Conducting similar cluster-based permutation tests on mu (μ; 8-12 Hz) and gamma (γ; 31-49 Hz) power revealed a significant negative cluster for μ power (t_{sum} = -4478.5, p = 0.001) centered around similar electrodes as for β power, though larger in size (CPz, CP1, CP3, Cz, C1, C3, FCz, FC1, FC3), but no significant cluster was found for γ power (t_{sum} < 221.5, p > 0.084).

These modulations were first quantified by averaging β-ERD over the entire delay period (-2 s to 0 s before go cue). The analysis revealed that the amplitude of β-ERD during the delay period was significantly influenced by Gauge ($F(2,60) = 7.7$, $p = 0.001$, $\eta^2p = 0.20$) but not by Target ($F(1,30) = 0.8$, $p = 0.368$, $\eta^2p = 0.03$), without any significant interaction between the two factors ($F(2,60) = 1.4$, $p = 0.265$, $\eta^2p = 0.04$). Post-hoc analysis revealed that the amplitude of β-ERD was significantly smaller for Med as compared to both Low ($t(30) = -3.1$, $p = 0.014$, $d = -0.55$) and High ($t(30) = -3.4$, $p = 0.006$, $d = -0.61$) but was not significantly different between Low and High ($t(30) = -1.0$, $p = 1.0$, $d = -0.17$) (Figure 3C, left panel). Note that β-ERD was computed by simply subtracting the average β power during a pre-cue baseline period (see Methods for details) to minimize transformation of the EEG signal, but other baseline corrections, such as percent signal change as proposed by Pfurtscheller and Lopes da Silva (1999) led to similar results (main effect of Target: $F(1,30) = 1.5$, $p = 0.225$, $\eta^2p = 0.05$; main effect of Gauge: $F(2,60) = 18.6$, $p = 10^{-6}$, $\eta^2p = 0.38$; interaction effect Target*Gauge: $F(2,60) = 1.3$, $p = 0.276$, $\eta^2p = 0.04$).

Interestingly, this Gauge effect was specific to modulations of β power as it was not found for μ power (Target: $F(1,30) = 0.1$, $p = 0.718$, $eta^2p = 0.00$; Gauge: $F(2,60) = 2.7$, $p = 0.078$, $eta^2p = 0.08$; Target*Gauge: $F(2,60) = 0.5$, $p = 0.621$, $eta^2p = 0.02$), or for γ power (Target:

466 $F(1,30) = 0.9$, $p = 0.355$, $eta^2p = 0.03$; Gauge: $F(2,60) = 1.8$, $p = 0.181$, $eta^2p = 0.06$;
467 Target*Gauge: $F(2,60) = 2.0$, $p = 0.141$, $eta^2p = 0.06$).

468 As the modulations of β power could have differently evolved across conditions throughout
469 a trial, a second analysis was run on the amplitude of β-ERD averaged over 500 ms temporal
470 windows, ranging from 2 to 0 s before go cue, therefore adding a Time factor to the analysis.
471 Consistent with the first analysis, neither a significant effect of Target was detected ($F(1,30) =$
472 0.8, $p = 0.367$, $\eta^2p = 0.03$), nor interactions between Target and Gauge ($F(2,60) = 1.3$, $p = 0.270$,
473 $\eta^2p = 0.04$), Target and Time ($F(3,90) = 1.0$, $p = 0.412$, $\eta^2p = 0.03$) and Target, Gauge and Time
474 ($F(6,180) = 1.6$, $p = 0.141$, $\eta^2p = 0.05$). However, consistent with the first analysis, significant
475 effects of Gauge ($F(2,60) = 7.6$, $p = 0.001$, $\eta^2p = 0.20$), Time ($F(3,90) = 25.6$, $p < 10^{-10}$, $\eta^2p =$
476 0.46), and an interaction between Gauge and Time ($F(6,180) = 5.9$, $p = 10^{-5}$, $\eta^2p = 0.16$) were
477 observed. Bonferroni-corrected t-tests conducted across Gauge and Time factors (12
478 comparisons) revealed the same pattern as in the first analysis, with significantly lower β-ERD
479 in Med as compared to Low and High, as early as 1.5 s before the go cue (Figure 3C, right
480 panel; Table 1).

481 Finally, β-ERD could also have differently evolved throughout blocks. Additional analysis
482 including a block factor showed a significant effect of Speed on β-ERD ($F(2,60) = 7.7$, $p =$
483 0.001; $eta^2p = 0.20$) but neither a significant effect of Target ($F(1,30) = 0.8$, $p = 0.367$, $eta^2p =$
484 0.03) nor Block ($F(1,30) = 0.2$, $p = 0.648$, $eta^2p = 0.01$). The analysis showed no significant
485 interaction with any of these factors ($F < 1.5$, $p > 0.234$, $eta^2p < 0.05$). Therefore, β-ERD does
486 not appear to have been differentially modulated across blocks.

487 **[Insert Figure 3]**

488 **[Insert Table 1]**

3. Action cost model

Considering the pattern of β-ERD found, we hypothesized that pre-movement modulations of β power might be best explained by changes in expected overall action cost, including both trajectory and temporal costs (Figure 1C, right panel; see Methods for details). This hypothesis assumed that action cost was lower in Med than High and Low conditions. Although at first glance the speed instructions of the present paradigm prevented participants from moving at the speed they preferred (i.e., that associated with the lowest cost), peak velocity distributions still revealed biases in participants' chosen speeds. Indeed, in spite of the very different average speeds reached across conditions (see behavioral results), most participants did not show trimodal distributions of peak velocities as would have been expected from the three non-overlapping peak velocity criteria used for each target. Instead, they oftentimes presented near-normal distributions, suggesting that their movement speeds were biased toward certain values. Indeed, even though speed instructions led to significantly different average speeds across conditions (Figure 2B), participants failed to perform their movements in the required criteria in a large proportion of trials (mean ± SD = 66.5 ± 8.2 %). Speed criteria were voluntarily strict enough to encourage participants to keep their speeds close to the speed criteria and therefore maximize speed differences across conditions. Still, we reasoned that inter-trial variability in movement speed could be exploited to estimate their speed preferences, especially considering that speed distributions appeared biased toward certain values for most participants. Hence, the peak velocity corresponding to the maximal value of probability density functions estimated from these distributions (based on kernel smoothing function for non-parametric distributions, see Methods for details) was used to estimate participants' preferred speed. The average estimated preferred peak velocity of movements toward Rt was 94.8 ± 13.7 cm/s. This value

was significantly lower than peak velocities found at HighRt ($t(30) = -11.0$, $p < 10^{-10}$, $d = -1.97$) and higher than peak velocities found at LowRt ($t(30) = 11.9$, $p < 10^{-10}$, $d = 2.15$), but interestingly was not significantly different from peak velocities at MedRt ($t(30) = -1.4$, $p = 0.178$, $d = -0.25$; Figure 4B, top panel). Likewise, estimated preferred peak velocities toward Lt were significantly lower than peak velocities found at HighLt ($t(30) = -8.0$, $p = 10^{-8}$, $d = -1.44$) and higher than peak velocities found at LowLt ($t(30) = 11.2$, $p < 10^{-10}$, $d = 2.01$), but not significantly different from peak velocities at MedLt ($t(30) = 0.4$, $p = 0.688$, $d = 0.07$; Figure 4B, bottom panel). The average estimated preferred peak velocity of movements toward Lt was 43.0 ± 10.0 cm/s. Together, these data indirectly confirm that although participants' preferred speed was not formally measured, it would have been close to the medium speed used here.

[Insert Figure 4]

The cost functions of movements directed toward Rt and Lt were estimated based on a model of action cost developed and applied to experimental data including reaching movements in previous work (Berret and Jean, 2016). This action cost model uses the combination of a trajectory cost which increases with movement speed and can be estimated based on task biomechanical constraints (e.g., angle and amplitude of the presented target, anthropometry, starting position of the arm), and a cost of time which decreases with movement speed and is estimated based on participants' preferred movement duration for a given amplitude. Because previous analysis of speed distributions showed that preferred speed estimates were not significantly different from the average speeds found in Med, average MTs in MedRt and MedLt were set as preferred movement durations in action cost models of movements directed to Rt and Lt respectively (see Methods for details and Figure 5A for illustration). Estimation of

peak velocity from the models appeared to fit the present data as the cost function of movements directed to Rt predicted optimal peak velocities (i.e., peak velocities corresponding to the minimum of the cost function; PrefRt) that were not significantly different from the average peak velocities found in MedRt ($t(30) = -1.1$, $p = 0.269$, $d = -0.20$, mean difference = -1.6 cm/s). Likewise, the cost function of movements directed to Lt predicted optimal peak velocities (PrefLt) that were not significantly different from average peak velocities found in MedLt ($t(30) = -0.3$, $p = 0.737$, $d = -0.06$, mean difference = -0.4 cm/s).

Critically, action cost predicted by the model followed a pattern close to the one found for β-ERD across conditions (Figure 5B). Once applied to the individual average peak velocity values found across conditions, estimated action cost from the model appeared significantly modulated by Target ($F(1,30) = 8.2$, $p = 0.008$, $\eta^2p = 0.21$), to a smaller extent than by Gauge ($F(2,60) = 38.6$, $p < 10^{-10}$, $\eta^2p = 0.56$), with a significant interaction between the two factors ($F(2,60) = 15.9$, $p = 10^{-6}$, $\eta^2p = 0.35$). Post-hoc analysis revealed a significantly lower estimated action cost in MedRt as compared to LowRt ($t(30) = -10.2$, $p = 10^{-10}$, $d = -1.83$) and to HighRt ($t(30) = -7.2$, $p = 10^{-7}$, $d = -1.30$), as well as in HighRt as compared to LowRt ($t(30) = -4.3$, $p = 0.001$, $d = 0.78$). Likewise, estimated action cost was significantly lower in MedLt as compared to LowLt ($t(30) = -9.4$, $p = 10^{-9}$, $d = -1.69$) and HighLt ($t(30) = -7.0$, $p = 10^{-6}$, $d = -1.26$), but not significantly different between HighLt and LowLt ($t(30) = 2.3$, $p = 0.268$, $d = 0.41$). Additionally, estimated action cost was significantly lower in HighLt in comparison to HighRt ($t(30) = 3.7$, $p = 0.007$, $d = 0.67$) but no significant difference was found when comparing MedLt to MedRt ($t(30) = 0.5$, $p = 1.0$, $d = 0.09$) and LowLt to LowRt ($t(30) = 0.3$, $p = 1.0$, $d = 0.06$).

Finally, a general linear mixed model (GLMM) was performed to test whether peak velocity and estimated action cost explained a significant proportion of the variance in β-ERD.

560 The model showed a significant influence of action cost ($F(1,154) = 8.5$, $p = 0.004$) but not of
561 peak velocity ($F(1,153) = 0.1$, $p = 0.823$) on β-ERD (Figure 5C). The results were similar when
562 including RTs in the model, with a significant influence of action cost on β-ERD ($F(1,153) =$
563 8.3, $p = 0.004$), but not of peak velocity ($F(1,154) = 0.2$, $p = 0.659$) or RTs ($F(1,179) = 1.5$, p
564 $= 0.223$). Therefore, modulations of pre-movement β-ERD across conditions appeared overall
565 better explained by changes in action cost rather than by the speed of movement initiation and
566 execution.

567 **[Insert Figure 5]**

Discussion

Using a speed-controlled reaching paradigm, the present study aimed to dissociate movement speed and action cost to determine which of these variables best explains changes in pre-movement β-ERD. Results showed that β-ERD was non-monotonically modulated by movement speed as its amplitude was greater both for slow and fast movements in comparison to movements performed at medium speed, following a u-shaped pattern. This pattern was observed for both targets despite very different ranges of speeds (~50-60 cm/s difference) and appeared specific to β power as it was not found when averaging activity in the μ and γ bands. Additionally, these modulations of β-ERD are unlikely to be explained by changes in movement accuracy or success in achieving the speed criteria considering that the two monotonically decreased with movement speed. Interestingly, GLMMs showed that β-ERD amplitude was better predicted by estimated action cost than by movement peak velocity or RT. As predicted by the model, the further the instructed speed from the optimal/preferred speed (i.e., speed associated with the lowest action cost), the greater the β-ERD. These results demonstrate that β-ERD constitutes a potential non-invasive marker of estimated action cost during motor planning.

To the best of our knowledge, this is the first report of a u-shaped association between β-ERD and movement speed. Indeed, β-ERD was attenuated at medium speeds but was comparatively larger both for slow and fast movements. While this observation appears somewhat incongruous with the association between β power and movement speed found in healthy individuals (Pogosyan et al., 2009) and in PD (Jenkinson and Brown, 2011), it is still consistent with some previous work that has reported no significant difference in β-ERD between slow and fast movements (Stancák and Pfurtscheller, 1995; Zhang et al., 2020; see Kilavik et al., 2013 for a review). The notion that beta reflects costs may offer an alternative

592 view reconciling the two. Namely, the amplitude of β-ERD might be modulated as a function
593 of action cost, therefore increasing both with movement time and effort considering that the
594 two are responsible for the devaluation of action (Berret and Jean, 2016; Shadmehr et al., 2016).
595 Consequently, greater β-ERD may facilitate the preparation of both slow and fast movements,
596 improving overall motor flexibility. Evidence for decreased speed when increasing β power
597 (Pogosyan et al, 2009) and increased speed when decreasing β power (Jenkinson and Brown,
598 2011) in the context of movements performed at maximal speed supports this hypothesis, but
599 facilitation of slow (i.e., slower than self-paced) movements does not appear to have been tested
600 yet. Furthermore, this assumption is consistent with the influential hypothesis that β power
601 favors the maintenance of the pre-existing neural state (Engel and Fries, 2010) as well as with
602 force production tasks, which typically reveal non-linear modulations of β power as a function
603 of exerted force (Tan et al., 2015; Fischer et al., 2019; Haddix et al., 2021). It also links the
604 attenuated β-ERD (Heinrichs-Graham et al., 2014) to the restricted motor repertoire observed
605 in PD (Baraduc et al., 2013; Sorrentino et al., 2021). From a neural perspective, this hypothesis
606 is supported by the known influence of β power on the flexibility of neuronal activity, β power
607 being considered as a marker of the excitation/inhibition balance in the primary motor cortex
608 (M1) (McAllister et al., 2013; Rossiter et al., 2014). Furthermore, the motor symptoms observed
609 in PD have been related to reduced plasticity in M1 (Bologna et al., 2018). This alteration of
610 motor flexibility and its associated β power increase might be linked to dopamine depletion
611 (Jenkinson and Brown, 2011), the action of dopamine being considered central in ensuring
612 behavioral flexibility (Jahanshahi et al., 2015; Cools, 2019).

613 The phasic dopaminergic activation preceding movement is modulated according to
614 expected action value in order to assess how much neural resources are worth allocating for an
615 upcoming movement (Hamid et al., 2016; Berke, 2018). Dopamine is thought to attenuate
616 signal-dependent noise, thereby allowing the formation of a more precise motor representation

(Manohar et al., 2015). This noise reduction process arguably requires additional neural computational power, which could be achieved through neuronal desynchronization. Indeed, β-ERD has been proposed as a mechanism allowing to increase the entropy of neuronal firing rates, resulting in an increase in their information coding capacity (Hanslmayr et al., 2012; Brittain and Brown, 2014). Beyond explaining the present results, the proposition of β-ERD as a marker of the allocation of neural resources unifies several lines of evidence. First, reward expectation is accompanied by an increase in β-ERD (Meyniel and Pessiglione, 2014; Savoie et al., 2019; Chen and Kwak, 2022). Given that reward is known to shift the speed-accuracy tradeoff of movements by increasing speed without penalizing accuracy (Manohar et al., 2015; Summerside et al., 2018), the greater β-ERD might reflect the allocation of additional neural resources to support the increase in speed. In this framework, the attenuation of beta-ERD observed in PD might be linked to a deficit in action valuation. This is supported by evidence of an alteration of effort-based decision-making and apathy in PD (Le Bouc et al, 2016). Second, motor learning has been associated with reduced sensorimotor activation over the course of practice, interpreted as a decrease in the mobilization of neural resources due to increased neural efficiency in the network (Karni et al., 1995; Kelly and Garavan, 2005). The amplitude of β-ERD has been shown to decrease with practice accordingly (Pollok et al., 2014; Gehringer et al., 2018). Third, this hypothesis also fits with the mounting evidence of β activity being modulated as a function of existing priors about stimuli and actions (Betti et al., 2021) because it may reflect the endogenous reactivation of these priors (Spitzer and Haegens, 2017). β-ERD might be attenuated when preparing movements at habitual speeds because of a stronger prior, which echoes the decrease in the amplitude of β-ERD found with learning.

The present results also offer a potential explanation for the cost of time implemented in models of action cost. Indeed, while the cost associated with fast movements can easily be justified by an increase of the net metabolic rate of movements with speed (Shadmehr et al.,

642 2016), what makes slow movements effortful is less clear (Berret and Jean, 2016). Nonetheless,
643 action selection can hardly be predicted from an energy minimization principle alone:
644 behavioral work has shown that movement duration impacts action choices independently from
645 changes in energy expenditure (Morel et al., 2017; Berret and Baud-Bovy, 2022). This influence
646 of movement duration on action selection has mostly been interpreted as the temporal
647 discounting of the rewarding value associated with the motor goal (Shadmehr et al., 2010; Choi
648 et al., 2014). Still, a temporal discounting of reward appears unlikely in the present task, given
649 that the reward consisted in reaching the speed criterion and was therefore intrinsically
650 associated with the slowing of movements. Furthermore, the positive correlation often reported
651 between the amplitude of β-ERD and expected reward (Meyniel and Pessiglione, 2014; Savoie
652 et al., 2019; Chen and Kwak, 2022) is inconsistent with a reduction of expected reward with
653 movement slowing in the present results. β-ERD amplitude at low speed was indeed
654 significantly greater than for medium speed, but not significantly different than for high speed.
655 Alternatively, in relation to the previous paragraph, this cost of time could be due to increased
656 neurocomputational demands or "neural effort" to perform slow movements. Indeed, slowing
657 down movements has been associated with an accumulation of constant noise (van Beers,
658 2008). Conversely, slow movements could be more costly simply because they are less often
659 performed. Movements at preferred speeds could be seen as a habitual form of control, which
660 is associated with lower computational cost due to an increased contribution of lower-order
661 brain regions (Schneider and Chein, 2003; Jahanshahi et al., 2015). In support, the motor cortex
662 has been shown to be less involved in habitual actions due to a preponderant role of the basal
663 ganglia (Kawai et al., 2015; Dhawale et al., 2021). Therefore, the magnitude of β-ERD could
664 be attenuated when preparing movements at preferred speeds because they require less
665 neocortical resources to be produced. This is consistent with evidence of spontaneous choices
666 of muscle coordination patterns favoring habits or less information encoding at the expense of

667 muscular effort or movement accuracy (de Rugy et al., 2012; Dounskaia and Shimansky, 2016).
668 However, preferred speeds were only approximated from distributions of speed values in the
669 present experiment because specific speed instructions were used in order to dissociate
670 movement speed from action cost. Additional studies measuring individualized preferred
671 speeds in a context of self-paced movements will be needed to confirm the existence of specific
672 modulation of β-ERD as a function of action cost.

673 In summary, the present results reconcile discrepancies concerning the relationship
674 between β-ERD and movement speed, and suggest that reducing β power facilitates the
675 preparation and execution of both fast and slow movements, by enhancing motor flexibility
676 through the allocation of additional neural resources. This encourages to explore the impact of
677 β power reduction in PD not only on movement speed, but also on action selection.

678

References

Baraduc P, Thobois S, Gan J, Broussolle E, Desmurget M (2013). A common optimization principle for motor execution in healthy subjects and parkinsonian patients. *J Neurosci* **33**:665–677.

Berke JD (2018). What does dopamine mean?. *Nat Neurosci* **21**:787–793.

Berret B, Baud-Bovy G (2022). Evidence for a cost of time in the invigoration of isometric reaching movements. *J Neurophysiol* **127**:689-701.

Berret B, Jean F (2016). Why Don't We Move Slower? The Value of Time in the Neural Control of Action. *J Neurosci* **36**:1056–1070.

Betti V, Della Penna S, de Pasquale F, Corbetta M (2021). Spontaneous Beta Band Rhythms in the Predictive Coding of Natural Stimuli. *Neuroscientist* **27**:184-201.

Bloem BR, Okun MS, Klein C (2021). Parkinson's disease. *Lancet* **397**:2284–2303.

Bologna M, Guerra A, Paparella G, Giordo L, Alunni Fegatelli D, Vestri AR, Rothwell JC, Berardelli A (2018). Neurophysiological correlates of bradykinesia in Parkinson's disease. *Brain* **141**:2432–2444.

Brittain JS, Brown P (2014). Oscillations and the basal ganglia: motor control and beyond. *Neuroimage* **85**:637–647.

Brittain JS, Sharott A, Brown P (2014). The highs and lows of beta activity in cortico-basal ganglia loops. *Eur J Neurosci* **39**:1951-9.

Chen XJ, Kwak Y (2022). Contribution of the sensorimotor beta oscillations and the cortico-basal ganglia-thalamic circuitry during value-based decision making: A simultaneous EEG-fMRI investigation. *Neuroimage* **257**:119300.

Choi JE, Vaswani PA, Shadmehr R (2014). Vigor of movements and the cost of time in decision making. *J Neurosci* **34**:1212–1223.

Cools R (2019). Chemistry of the Adaptive Mind: Lessons from Dopamine. *Neuron* **104**:113–131.

Delorme A, Makeig S (2004). EEGLAB: an open source toolbox for analysis of single-trial EEG dynamics including independent component analysis. *J Neurosci Methods* **134**:9–21.

de Rugy A, Loeb GE, Carroll TJ (2012). Muscle coordination is habitual rather than optimal. *J Neurosci* **32**:7384–7391.

Dhawale AK, Wolff S, Ko R, Ölveczky BP (2021). The basal ganglia control the detailed kinematics of learned motor skills. *Nat Neurosci* **24**:1256–1269.

Dounskaia N, Shimansky Y (2016). Strategy of arm movement control is determined by minimization of neural effort for joint coordination. *Exp Brain Res* **234**:1335–1350.

Engel AK, Fries P (2010). Beta-band oscillations--signalling the status quo?. *Curr Opin Neurobiol* **20**:156–165.

Fischer AG, Nigbur R, Klein TA, Danielmeier C, Ullsperger M (2018). Cortical beta power reflects decision dynamics and uncovers multiple facets of post-error adaptation. *Nat Commun* **9**:5038.

Fischer P, Pogosyan A, Green AL, Aziz TZ, Hyam J, Foltynie T, Limousin P, Zrinzo L, Samuel M, Ashkan K, Da Lio M, De Cecco M, Fornaser A, Brown P, Tan H (2019). Beta synchrony in the cortico-basal ganglia network during regulation of force control on and off dopamine. *Neurobiol Dis* **127**:253–263.

Flash T, Hogan N (1985). The coordination of arm movements: an experimentally confirmed mathematical model. *J Neurosci* **5**:1688–1703.

Fries P (2015). Rhythms for Cognition: Communication through Coherence. *Neuron* **88**:220-35.

Gehringer JE, Arpin DJ, Heinrichs-Graham E, Wilson TW, Kurz MJ (2018). Neurophysiological changes in the visuomotor network after practicing a motor task. *J Neurophysiol* **120**:239–249.

Gordon J, Ghilardi MF, Cooper SE, Ghez C (1994). Accuracy of planar reaching movements. II. Systematic extent errors resulting from inertial anisotropy. *Exp Brain Res* **99**:112–130.

Gottlieb GL, Corcos DM, Agarwal GC (1989). Organizing principles for single-joint movements. I. A speed-insensitive strategy. *J Neurophysiol* **62**:342–357.

Grent-'t-Jong T, Oostenveld R, Jensen O, Medendorp WP, Praamstra P (2013). Oscillatory dynamics of response competition in human sensorimotor cortex. *Neuroimage* **83**:27-34.

Haddix C, Al-Bakri AF, Sunderam S (2021). Prediction of isometric handgrip force from graded event-related desynchronization of the sensorimotor rhythm. *J Neural Eng* **18**: 10.1088/1741-2552/ac23c0.

Hamid AA, Pettibone JR, Mabrouk OS, Hetrick VL, Schmidt R, Vander Weele CM, Kennedy RT, Aragona BJ, Berke JD (2016). Mesolimbic dopamine signals the value of work. *Nat Neurosci* **19**:117–126.

Hanslmayr S, Staudigl T, Fellner MC (2012). Oscillatory power decreases and long-term memory: the information via desynchronization hypothesis. *Front Hum Neurosci* **6**:74.

Heinrichs-Graham E, Wilson TW, Santamaria PM, Heithoff SK, Torres-Russotto D, Hutter-Saunders JA, Estes KA, Meza JL, Mosley RL, Gendelman HE (2014). Neuromagnetic evidence of abnormal movement-related beta desynchronization in Parkinson's disease. *Cereb Cortex* **24**:2669–2678.

Jahanshahi M, Obeso I, Rothwell JC, Obeso JA (2015). A fronto-striato-subthalamic-pallidal network for goal-directed and habitual inhibition. *Nat Rev Neurosci* **16**:719–732.

Jenkinson N, Brown P (2011). New insights into the relationship between dopamine, beta oscillations and motor function. *Trends Neurosci* **34**:611–618.

Jung TP, Makeig S, Humphries C, Lee TW, McKeown MJ, Iragui V, Sejnowski TJ (2000). Removing electroencephalographic artifacts by blind source separation. *Psychophysiology* **37**:163–178.

Karni A, Meyer G, Jezzard P, Adams MM, Turner R, Ungerleider LG (1995). Functional MRI evidence for adult motor cortex plasticity during motor skill learning. *Nature* **377**:155–158.

Kawai R, Markman T, Poddar R, Ko R, Fantana AL, Dhawale AK, Kampff AR, Ölveczky BP (2015). Motor cortex is required for learning but not for executing a motor skill. *Neuron* **86**:800–812.

Kelly AM, Garavan H (2005). Human functional neuroimaging of brain changes associated with practice. *Cereb Cortex* **15**:1089–1102.

Kilavik BE, Zaepffel M, Brovelli A, MacKay WA, Riehle A (2013). The ups and downs of β oscillations in sensorimotor cortex. *Exp Neurol* **245**:15–26.

Kühn AA, Kupsch A, Schneider GH, Brown P (2006). Reduction in subthalamic 8-35 Hz oscillatory activity correlates with clinical improvement in Parkinson's disease. *Eur J Neurosci* **23**:1956–1960.

Le Bouc R, Rigoux L, Schmidt L, Degos B, Welter ML, Vidailhet M, Daunizeau J, Pessiglione M (2016). Computational Dissection of Dopamine Motor and Motivational Functions in Humans. *J Neurosci* **36**:6623-33.

Manohar SG, Chong TT, Apps MA, Batla A, Stamelou M, Jarman PR, Bhatia KP, Husain M (2015). Reward Pays the Cost of Noise Reduction in Motor and Cognitive Control. *Curr Biol* **25**:1707–1716.

McAllister CJ, Rönnqvist KC, Stanford IM, Woodhall GL, Furlong PL, Hall SD (2013). Oscillatory beta activity mediates neuroplastic effects of motor cortex stimulation in humans. *J Neurosci* **33**:7919–7927.

Meyniel F, Pessiglione M (2014). Better get back to work: a role for motor beta desynchronization in incentive motivation. *J Neurosci* **34**:1–9.

Morel P, Ulbrich P, Gail A (2017). What makes a reach movement effortful? Physical effort discounting supports common minimization principles in decision making and motor control. *PLoS Biol* **15**:e2001323.

Oostenveld R, Fries P, Maris E, Schoffelen JM (2011). FieldTrip: Open source software for advanced analysis of MEG, EEG, and invasive electrophysiological data. *Comput Intell Neurosci* **2011**:156869.

Pfurtscheller G, Lopes da Silva FH (1999). Event-related EEG/MEG synchronization and desynchronization: basic principles. *Clin Neurophysiol* **110**:1842–1857.

Pogosyan A, Gaynor LD, Eusebio A, Brown, P (2009). Boosting cortical activity at Beta-band frequencies slows movement in humans. *Curr Biol* **19**:1637–1641.

Pollok B, Latz D, Krause V, Butz M, Schnitzler A (2014). Changes of motor-cortical oscillations associated with motor learning. *Neuroscience* **275**:47–53.

Ray NJ, Jenkinson N, Wang S, Holland P, Brittain JS, Joint C, Stein JF, Aziz T (2008). Local field potential beta activity in the subthalamic nucleus of patients with Parkinson's disease is associated with improvements in bradykinesia after dopamine and deep brain stimulation. *Exp Neurol* **213**:108–113.

Rossiter HE, Davis EM, Clark EV, Boudrias MH, Ward NS (2014). Beta oscillations reflect changes in motor cortex inhibition in healthy ageing. *Neuroimage* **91**:360–365.

Savoie FA, Hamel R, Lacroix A, Thénault F, Whittingstall K, Bernier PM (2019). Luring the Motor System: Impact of Performance-Contingent Incentives on Pre-Movement Beta-Band Activity and Motor Performance. *J Neurosci* **39**:2903–2914.

Schneider W, Chein JM (2003). Controlled & automatic processing: behavior, theory, and biological mechanisms. *Cogn Sci* **27**:525-559.

Scrivener CL, Reader AT (2022). Variability of EEG electrode positions and their underlying brain regions: visualizing gel artifacts from a simultaneous EEG-fMRI dataset. *Brain Behav* **12**:e2476.

Shadmehr R, Huang HJ, Ahmed AA (2016). A Representation of Effort in Decision-Making and Motor Control. *Curr Biol* **26**:1929–1934.

Shadmehr R, Orban de Xivry JJ, Xu-Wilson M, Shih TY (2010). Temporal discounting of reward and the cost of time in motor control. *J Neurosci* **30**:10507–10516.

Sorrentino P, Rucco R, Baselice F, De Micco R, Tessitore A, Hillebrand A, Mandolesi L, Breakspear M, Gollo LL, Sorrentino G (2021). Flexible brain dynamics underpins complex behaviours as observed in Parkinson's disease. *Sci Rep* **11**(1):4051.

Spitzer B, Haegens S (2017). Beyond the Status Quo: A Role for Beta Oscillations in Endogenous Content (Re)Activation. *eNeuro* **4**:ENEURO.0170-17.2017.

816 Stancák A Jr, Pfurtscheller G (1995). Desynchronization and recovery of beta rhythms
817 during brisk and slow self-paced finger movements in man. *Neurosci Lett* **196**:21-4.

818 Summerside EM, Shadmehr R, Ahmed AA (2018). Vigor of reaching movements:
819 reward discounts the cost of effort. *J Neurophysiol* **119**:2347–2357.

820 Takemi M, Masakado Y, Liu M, Ushiba J (2013). Event-related desynchronization
821 reflects downregulation of intracortical inhibition in human primary motor cortex. *J*
822 *Neurophysiol* **110**:1158-66.

823 Tan H, Pogosyan A, Ashkan K, Cheeran B, FitzGerald JJ, Green AL, Aziz T, Foltynie
824 T, Limousin P, Zrinzo L, Brown P (2015). Subthalamic nucleus local field potential activity
825 helps encode motor effort rather than force in parkinsonism. *J Neurosci* **35**:5941–5949.

826 van Beers RJ (2008). Saccadic eye movements minimize the consequences of motor
827 noise. *PloS One* **3**:e2070.

828 Wach C, Krause V, Moliadze V, Paulus W, Schnitzler A, Pollok B (2013). Effects of
829 10 Hz and 20 Hz transcranial alternating current stimulation (tACS) on motor functions and
830 motor cortical excitability. *Behav Brain Res* **241**:1-6.

831 Wiesman AI, Koshy SM, Heinrichs-Graham E, Wilson TW (2020). Beta and gamma
832 oscillations index cognitive interference effects across a distributed motor network.
833 *Neuroimage* **213**:116747.

834 Young SJ, Pratt J, Chau T (2009). Target-directed movements at a comfortable pace:
835 movement duration and Fitts's law. *J Mot Behav* **41**:339–346.

836 Yuan H, Liu T, Szarkowski R, Rios C, Ashe J, He B (2010). Negative covariation
837 between task-related responses in alpha/beta-band activity and BOLD in human sensorimotor
838 cortex: an EEG and fMRI study of motor imagery and movements. *Neuroimage* **49**:2596-606.

839 Zhang X, Li H, Xie T, Liu Y, Chen J, Long J (2020). Movement speed effects on beta-
840 band oscillations in sensorimotor cortex during voluntary activity. *J Neurophysiol* **124**:352-
841 359.

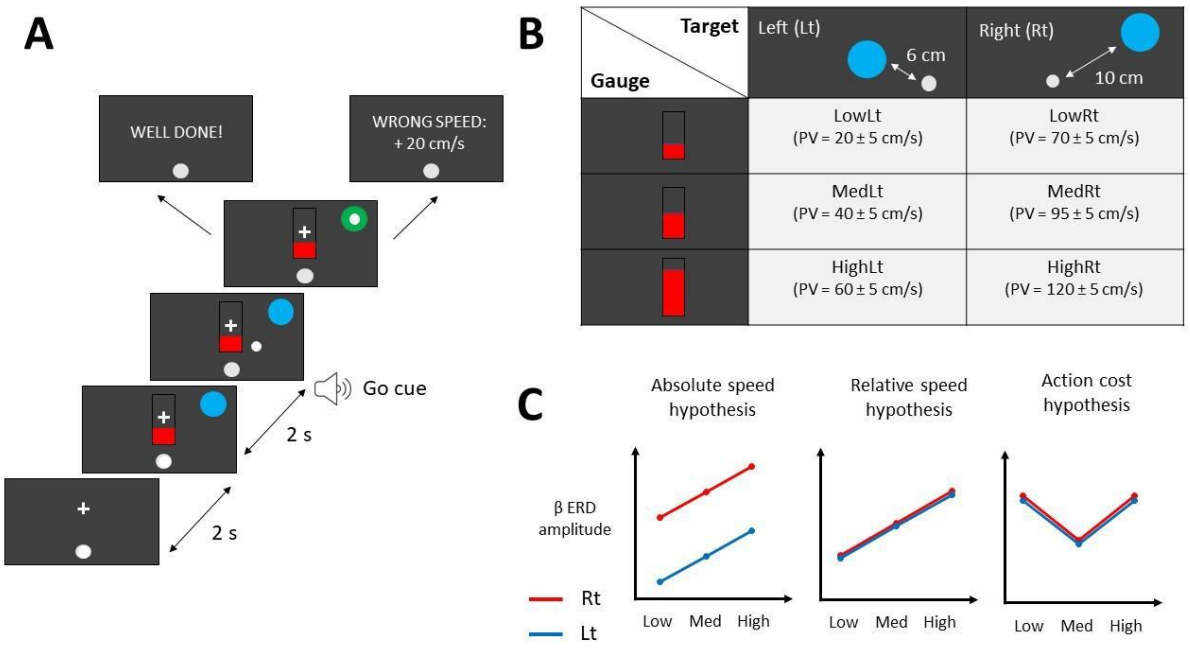

842 **Figure 1. Methods. A**: Schematic representation of a trial timeline. The content of each dark
843 grey rectangle illustrates stimuli that were displayed on the screen in front of participants. The
844 trial started with the appearance of a white fixation cross at the center of the screen and the
845 starting base (light grey circle; bottom rectangle). Once participants had kept the cursor (white
846 circle) inside of the starting base for 2 s, the target (blue circle) and the gauge appeared on the
847 screen. Participants were asked to reach the target once they heard the go cue, which occurred
848 2 s after the appearance of the gauge and the target on the screen. Once the target was hit, it
849 turned green. Written feedback was then given to participants about whether their movement
850 reached the speed criterion. **B**: Summary of the speed criteria across conditions. The table
851 indicates the intervals of peak velocities (PV) that participants were asked to reach according
852 to the position of the presented target (columns) and the filling level of the gauge (rows). **C**:
853 Working hypotheses of what patterns of β-ERD across conditions could be expected from
854 modulations of movement speed. Conditions including movements directed to Rt are
855 represented in red and conditions including movements toward Lt are in blue.

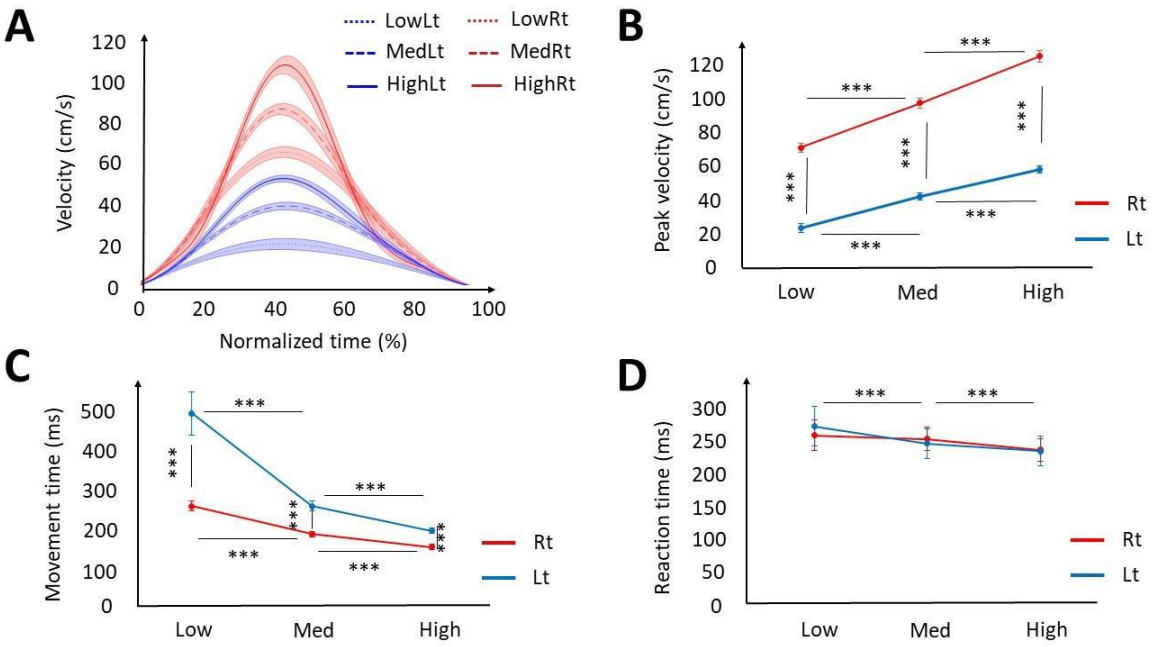

Figure 2. Behavioral results. Red and blue lines/dots refer to Rt and Lt respectively. **A**: Average normalized velocity profiles across conditions. Solid lines refer to High, large dotted lines to Med and small dotted lines to Low conditions. **B, C, D**: Average peak velocities, MTs and RTs across conditions. Error bars indicate 95% confidence intervals around the mean. *** $p < 0.001$

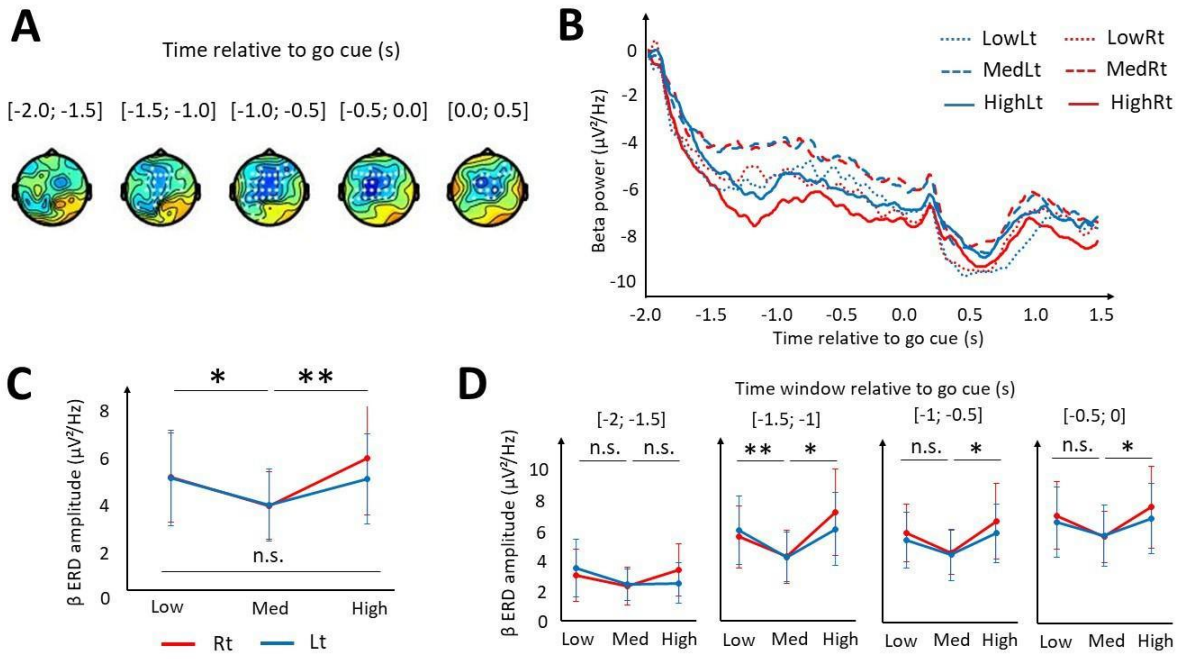

Figure 3. Modulations of β power across conditions. **A**: Illustration of the results from cluster-based permutation tests. Each topographical plot represents the average difference in β power between conditions requiring the slowest (LowLt) and the fastest (HighRt) movements in 500-ms windows, time-locked to the occurrence of the go cue. Hot colors indicate an increase and cold colors a decrease in β power. White dots indicate electrodes belonging to a significant cluster. **B**: Time course of average β power change from baseline throughout a trial. **C**: Average β-ERD amplitude during the delay period (2 s preceding go cue). Red and blue lines/dots indicate results from movements directed to Rt and Lt respectively. **D**: Similar representations to C, with β power averaged in 500-ms windows encompassing the delay period. Error bars indicate 95% confidence intervals around the mean. ** $p < 0.01$, * $p < 0.05$

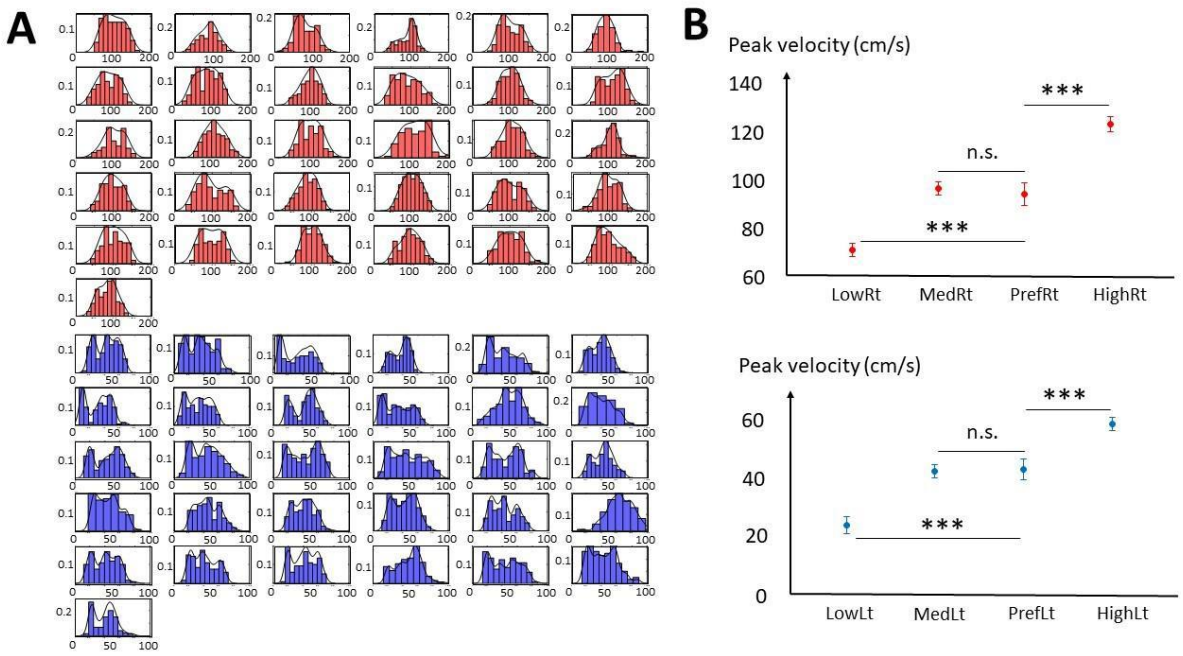

Figure 4. Peak velocity distributions and probability density functions across participants. **A**: Peak velocity distributions. Red histograms represent peak velocities of movements toward Rt, and blue histograms peak velocities of movements toward Lt. Each histogram represents data from one participant. Y-axis indicates the normalized proportion of trials (from 0 to 1) and x-axis the peak velocities. The solid black curve represents an estimate of the probability density function of each distribution. **B**: Comparison of the average estimated preferred peak velocity (PrefRt and PrefLt; determined using the maximum of probability density functions illustrated in A) to the average peak velocities of the different experimental conditions. Red and blue dots refer to Rt and Lt respectively. Error bars indicate 95 % confidence intervals around the mean. *** $p < 0.001$

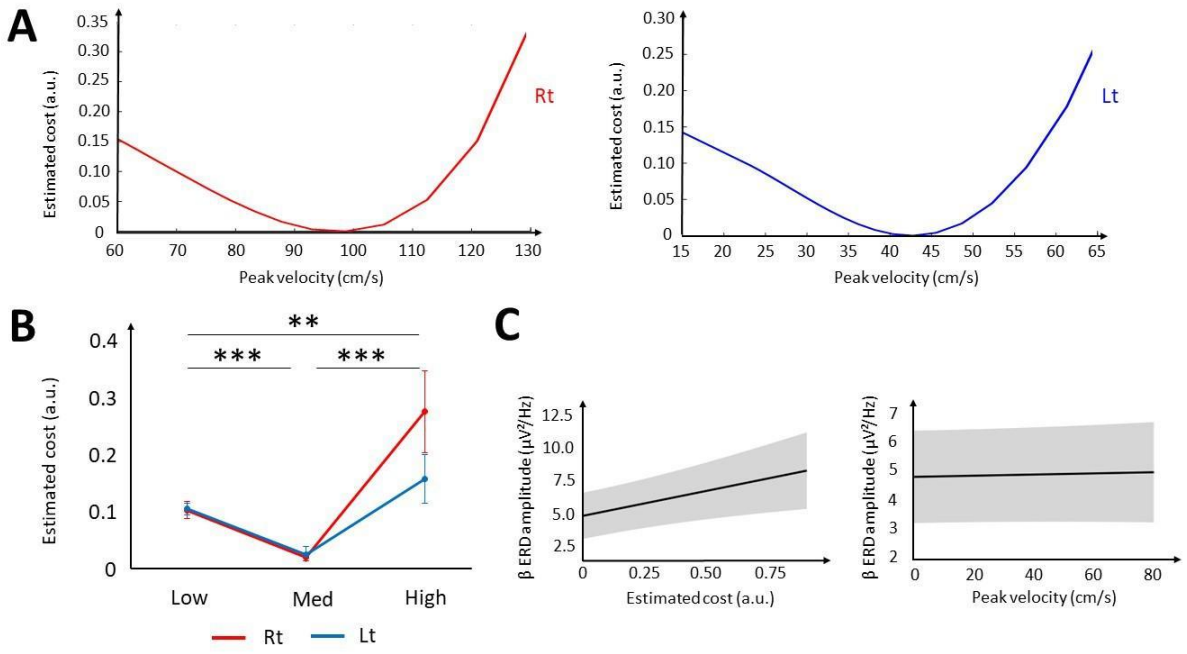

876 **Figure 5. Results from the modeling of action cost. A**: Representations of the estimated cost
877 computed by the model as a function of peak velocities (top panels) and MT (bottom panels).
878 The cost of movements directed to Rt is illustrated with red curves (left panels) and the cost of
879 movements directed to Lt with blue curves (right panels). **B**: Estimated costs of movements
880 directed to Rt (red) and Lt (blue) across speed conditions. **C**: Representation of the correlation
881 between β-ERD amplitude and normalized estimated cost (left panel) and peak velocity (right
882 panel) based on the estimated marginal means computed by the GLMM. Error bars (B) or
883 shaded areas (C) indicate 95 % confidence intervals. ** $p < 0.01$, *** $p < 0.001$

Time window (relative to go cue)	Contrast	T-statistic	P-value (Bonferroni-corrected)	Effect size (Cohen's d)
[-2 to -1.5 s]	Low vs Med	2.2	0.462	0.39
	Low vs High	0.8	1.0	0.14
	Med vs High	-1.9	0.798	-0.34
[-1.5 to -1 s]	Low vs Med	3.8	**0.007**	0.69
	Low vs High	-1.6	1.0	-0.29
	Med vs High	-3.5	**0.017**	-0.63
[-1 to -0.5 s]	Low vs Med	2.9	0.092	0.51
	Low vs High	-1.2	1.0	-0.22
	Med vs High	-3.7	**0.01**	-0.67
[-0.5 to 0 s]	Low vs Med	2.8	0.119	0.49
	Low vs High	1.0	1.0	0.18
	Med vs High	-3.3	**0.031**	-0.59

884 **Table 1. Results from post-hoc analysis on β power across speed conditions and time**

885 **bins**. P-values inferior to 0.05 are in bold.